Ballistic thermal transport coupled to phonons

Panagiotis Zavitsanos

September 11, 2020

Under the direction of Xenophon Zotos

Dept. of Physics
University of Crete

1 Introduction

In recent years there has been interest in magnetic materials and the particular mechanisms by which heat is transported in them as transport phenomena provide valuable information on material excitations and interactions.Other than the familiar lattice excitations it has been observed that in some of them, propagating excitations of the spin system known as magnons have a noticable effect on heat propagation.Experimentally any contributions made to the measured $effective$ conductivity by the magnon system , can only be indirectly addressed considering that the phonon temperature is the only one directly measured.As a result study of phonon-magnon coupling is of great importance as it sheds light on basic thermal properties and builds a better understanding of their overall interaction.

Attention has been drawn to antiferromagnetic Heisenberg spin chain (SC) and certain spin ladder (SL) materials due to the large heat conductivities observed.For a SC material such an observation is understandable as ballistic heat transport is expected [1] to occur along the chain axis through magnetic topological excitations called spinons. Contrary for a SL material such a behaviour is quite peculiar as magnetic heat transport by "triplon" excitations is expected to be dissipative [2].Both materials are electrical insulators so we can safely exclude electrons from heat transport and consider phonons and spin excitations as the main heat carriers.

The experimental techniques involved in the evaluation of the thermal conductivity of the forementioned materials include a steady state method (SSM) and a fluorescent flash method (FFM)[3].For the SSM steady heat flow is achieved by heating one front of the material and taking temperature measurements at both ends.The analysis involved in the SSM was carried by Sanders and Walton [4] and has become a standard way of measuring thermal conductivity.The FFM method is a dynamic one.The material is coated with a fluorescent layer and then heated with a laser pulse.Surface phonons interact with the layer and produce light allowing time tracking of the temperature evolution.In that case heat transport is described by a two-temperature (2T) model :

$$\begin{aligned} C_p\partial_t T_p &= k_p\partial_x^2 T_p - g(T_p - T_m) \\ C_m\partial_t T_m &= k_m\partial_x^2 T_m - g(T_m - T_p) \end{aligned} \tag{1}$$

where t is time , x is the coordinate along the chain or ladder axis $T_{p,m}$, $C_{p,m}$, $k_{p,m}$ are the temperature , specific heat , thermal conductivity of the lattice and magnetic subsystems, $g = C_pC_m/[(C_p + C_m)\tau]$ is the coupling constant and τ is a time constant that is related to the energy exchange rate between the two systems.

Such experiments have been conducted on the magnetically gapless SC $SrCuO_2$ and on the gapped cuprate $Ca_9La_5Cu_{24}O_{41}$ [5].Analytic solutions of (1) make an evaluation of τ possible through proper fitting of the experimental values of $C_{p,m}$, $k_{p,m}$.It is found that $\tau_{(SC)} \approx (1 \pm 1) \times 10^{-12}s$ whereas $\tau_{(SL)} \approx (4 \pm 1) \times 10^{-4}s$.The spin ladder relaxation time is 8 orders of magnitude slower than the corresponding spin chain value.It is one of the longest phonon magnon thermalization times measured comparable only to 3D antiferromagnets such as MnF_2.This discrepancy can be explained by spin conservation arguments where a two-magnon one-phonon scattering occurs.Equation (1) is consistent with the diffusive nature of magnon heat transport in a SL material but completely fails to model the ballistic character of an SC material.

Below heat propagation will be discussed in the context of a ballistic magnetic component.At first new equations to model such behaviour are given.Additionally analytical solutions for the $effective$ thermal conductivity of the steady state case will be derived and a numerical approach to the related dynamics will be performed.

2 Model Equations

In the model below temperature evolution of the system depends only on the phonon and spinon subsystems.Each one has a temperature T_p , T_m.Diffusive behaviour is assumed for the phonon system and ballistic for the magnetic one.Additionally

the spinon subsystem consists of right and left travelling magnetic heat carriers. According to Sanders and Walton the temperature difference between phonons (T_p) and spinons (T_m) comes to an equilibrium.

$$\frac{\partial \Delta T}{\partial t} = -\frac{\Delta T}{\tau}, \quad \Delta T = T_p - T_m. \tag{2}$$

The individual contributions of the two subsystems are

$$\begin{aligned} \frac{\partial T_p}{\partial t} &= \frac{c_m}{C}\frac{T_m - T_p}{\tau} \\ \frac{\partial T_+}{\partial t} &= \frac{c_p}{C}\frac{T_p - T_+}{\tau} \\ \frac{\partial T_-}{\partial t} &= \frac{c_p}{C}\frac{T_p - T_-}{\tau} \end{aligned} \tag{3}$$

where $T_\pm$ is the temperature of the right and left moving carriers , $T_m = (T_+ + T_-)/2$, $c_m = (c_+ + c_-)$ the associated specific heat , c_p the phonon specific heat , $C = c_p + c_m$ and τ a relaxation time between the two systems.

Equations (3) describe the energy exchange between the subsystems but provide no information on the spatial dependence of the temperature distribution.To achieve this a diffusion equation is used for the phonon system and an advection for the spinon one.The later being the choice for ballistic behaviour as solutions are travelling waves and the advected quantity is conserved.As ballistic transport occurs along the chain axis in SC materials , only one spatial dimension is taken into account.We have :

$$\begin{aligned} \frac{\partial \epsilon_p}{\partial t} &= D\frac{\partial^2 \epsilon_p}{\partial x^2} + \frac{c_p c_m}{C}\frac{T_m - T_p}{\tau} \\ \frac{\partial \epsilon_\pm}{\partial t} \pm v\frac{\partial \epsilon_\pm}{\partial x} &= \frac{c_p c_\pm}{C}\frac{T_p - T_\pm}{\tau} \end{aligned} \tag{4}$$

where D is the phonon diffusion constant and v the velocity of magnetic excitations. We find the phonon (Q_p) and magnetic (Q_m) energy currents to be $Q_p = -\kappa_p \frac{\partial T_p}{\partial x}$, $Q_m = v\epsilon_+ - v\epsilon_-$.Going back to temperature dependent equations we have

$$\begin{aligned} &\frac{\partial T_p}{\partial t} = D\frac{\partial^2 T_p}{\partial x^2} + \frac{c_m}{C}\frac{T_m - T_p}{\tau} \\ &\frac{\partial T_\pm}{\partial t} \pm v\frac{\partial T_\pm}{\partial x} = \frac{c_p}{C}\frac{T_p - T_\pm}{\tau} \\ &Q = Q_p + Q_m = -\kappa_p\frac{\partial T_p}{\partial x} + v\frac{c_m}{2}(T_+ - T_-). \end{aligned} \tag{5}$$

3 Steady state analysis

Assuming steady heat flow the equations become

$$\begin{aligned} v\frac{\partial T_m}{\partial x} &= -\frac{c_p}{C}\frac{\Delta T_m}{\tau} \\ D\frac{\partial^2 T_p}{\partial x^2} + \frac{c_m}{C}\frac{T_m - T_p}{\tau} &= 0 \end{aligned} \tag{6}$$

$$Q = -\kappa_p\frac{\partial T_p}{\partial x} + v c_m \Delta T_m \quad , \quad \Delta T_m = \frac{T_+ - T_-}{2}. \tag{7}$$

To solve we consider a system $-L/2 < x < L/2$ with only phonon energy currrent $Q|_{x=\pm L/2} = Q_p$ at its borders and no magnetic current $(T_+ - T_-)|_{x=\pm L/2} = 0$.

Solving (7) for ΔT_m and substituting in (6) we get

$$\frac{\partial T_m}{\partial x} = \frac{c_p}{c_m}\frac{1}{Cv^2\tau}(Q + \kappa_p\frac{\partial T_p}{\partial x})$$

The quantity $Cv^2\tau$ has thermal conductivity units so $\kappa = Cv^2\tau$ defines an effective "transfer thermal conductivity".The above equation becomes

$$\frac{\partial T_m}{\partial x} = -\frac{c_p}{c_m}\frac{1}{\kappa}(Q + \kappa_p\frac{\partial T_p}{\partial x}) \tag{8}$$

Equation (8) is easily integrated , provided that c_p , c_m are temperature independent and that the boundary condition $T_p(x=0) = T_m(0) = T_0$ is satisfied.We find

$$T_m = T_0 - \frac{c_p}{c_m}\frac{1}{\kappa}Qx - \frac{c_p}{c_m}\frac{\kappa_p}{\kappa}(T_p - T_0) \tag{9}$$

Substituting (9) in (8) we have

$$\begin{aligned} &\frac{\partial^2(T_p - T_0)}{\partial x^2} - A^2(T_p - T_0) - Qx = 0 \\ &A^2 = \frac{1}{C\tau}(\frac{c_p c_m}{\kappa_p} + \frac{c_p^2}{\kappa}) \\ &B = \frac{1}{C\tau}\frac{c_p^2}{\kappa\kappa_p}. \end{aligned} \tag{10}$$

Solving this equation with the boundary condition $\partial(T_p - T_0)/\partial x = -Q/\kappa_p$ gives the phonon temperature profile

$$T_p = T_0 - (\frac{Bx}{A^2} - \frac{(B/A^2 - 1/\kappa_p)\sinh Ax}{A\cosh AL/2})Q \tag{11}$$

and by substitution of the above to (9) the magnetic one.
If $\tau \to 0$ then $A \to \infty$.At this limit the last term of eq. (11) tends to zero , so

$$T_p(x) \to T_0 - \frac{BQ}{A^2}x$$

For a two-diffusion model

$$T_p(x) \to T_0 - \frac{Q}{(\kappa_m + \kappa_p)}x$$

Knowing the form of the static temperature profile in the context of a two-diffusion model enables a direct comparison with the advection-diffusion one. Considering the above limit , the static temperature profile can be plotted for the spin ladder ($Ca_9La_5Cu_{24}O_2$) and spin chain ($SrCuO_2$) materials using the parameter values listed in Table 1.

TABLE I.Parameter values used in Figures 1,2.

Quantity	Spin ladder	Spin chain	Dimensions
c_m	$2,8 \times 10^6$	$2,8 \times 10^6$	$JK^{-1}m^{-3}$
c_p	$1,5 \times 10^5$	3×10^4	$JK^{-1}m^{-3}$
κ_p	1	8	$WK^{-1}m^{-1}$
κ_m	45	40	$WK^{-1}m^{-1}$
τ	4×10^{-4}	10^{-12}	s
v	$-$	2×10^4	ms^{-1}

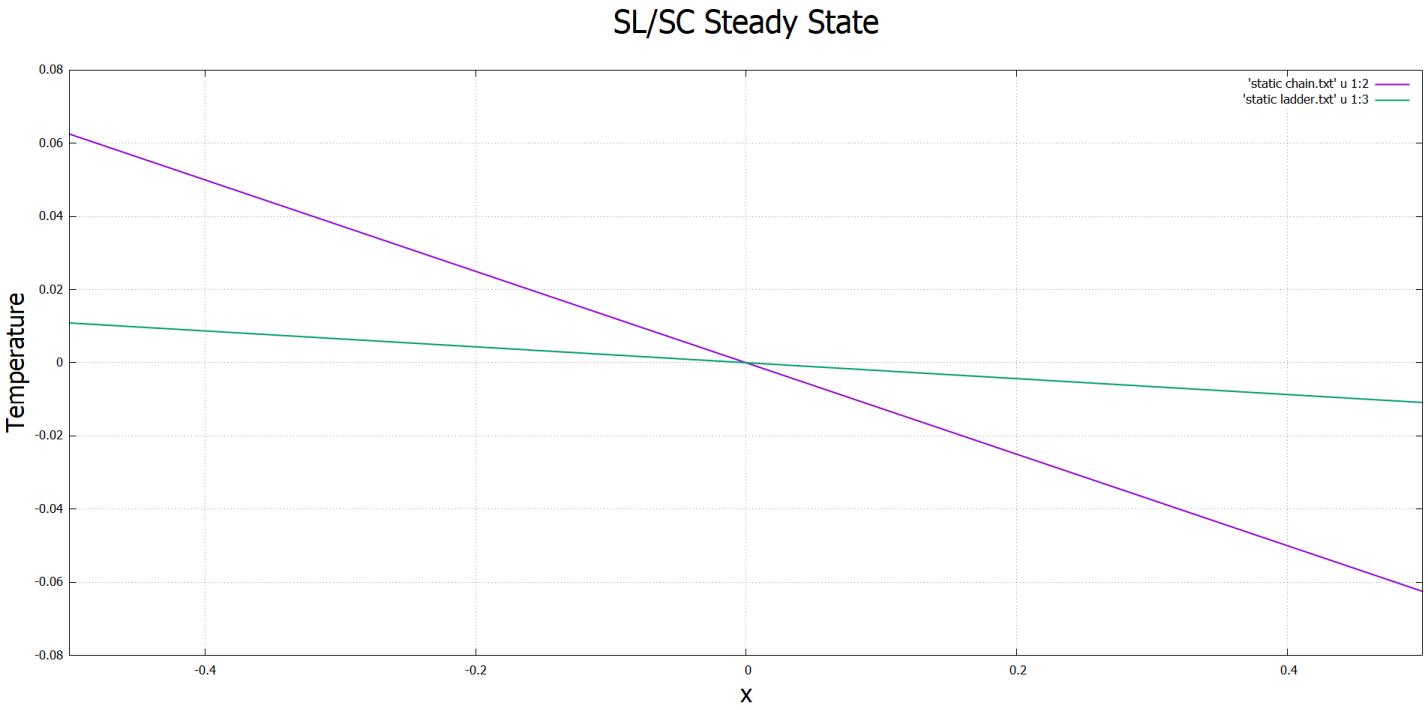

Figure 1: Green: Spin ladder / Purple: Spin chain

The temperature profile for each material is plotted in accordance with the corresponding model.

4 Effective thermal conductivity

In a SSM thermal conductivity experiment the temperature difference between the two ends of the sample $\Delta T_p = T(L/2) - T(-L/2)$ can be measured.Knowing the heat flux supplied , the effective thermal conductivity is calculated from

$$\kappa_{eff} = -QL/\Delta T_p = \frac{1}{\frac{B}{A^2} - \frac{B/A^2 - 1/\kappa_p}{AL}\tanh(AL/2)}. \tag{12}$$

To better understand this relation we approximate heat capacity as $c_m \sim T_0/v$, $c_p \sim T_0/v_p$ with v_p being a characteristic phonon velocity and $v_p << v$.

$$\begin{aligned} \frac{B}{A^2} &= \frac{1}{\kappa_p + \kappa\frac{c_m}{c_p}} \sim \frac{1}{T_0(l_p + l)} \\ \frac{1}{\kappa_p} &\sim \frac{1}{T_0 l_p}, \end{aligned} \tag{13}$$

with $c_m << c_p$, $\kappa_p = c_p v_p l_p$ and $l = v\tau$. In the above limit,

$$\begin{aligned} AL &\sim \sqrt{\frac{L^2}{l}(\frac{1}{l} + \frac{1}{l_p})} \\ \kappa_{eff} &\sim \frac{T_0}{\frac{1}{l+l_p} - (\frac{1}{l+l_p} - \frac{1}{l_p})\frac{\tanh(AL/2)}{AL}} \\ \kappa_{eff} &\sim \frac{T_0}{\frac{1}{l+l_p} + \frac{1}{l_p}}, \quad AL \to 0 \\ \kappa_{eff} &\sim T_0(l + l_p) \sim \kappa_p + \kappa, \quad AL \to \infty \end{aligned} \tag{14}$$

5 Dynamic approach

As the FFM method allows us to observe the temperature evolution of the phonon system it is useful to revisit the time dependent equations of the model.

$$\frac{\partial T_p}{\partial t} = D\frac{\partial^2 T_p}{\partial x^2} + \frac{c_m}{C}\frac{T_m - T_p}{\tau}$$
$$\frac{\partial T_\pm}{\partial t} \pm v\frac{\partial T_\pm}{\partial x} = \frac{c_p}{C}\frac{T_p - T_\pm}{\tau}$$

For an open system of length L with zero energy current boundary conditions , $Q_p = 0 \Rightarrow \frac{\partial T_p}{\partial x}|_{x=0,L} = 0$, $Q_m = 0 \Rightarrow T_+|_{x=0,L} = T_-|_{x=0,L}$. Due to difficulties that arise when applying many of the standard computational methods in order to solve an advection equation a Fourier approximation is preferred. Assuming solutions of the form

$$\begin{aligned} T_p &= \frac{a_0}{2} + \sum_{n=1}^{+\infty} a_n \cos q_n x, \quad q_n = \frac{\pi n}{L} \\ T_\pm &= \frac{b_0}{2} + \sum_{n=1}^{+\infty} b_n \cos q_n x \pm c_n \sin q_n x. \end{aligned} \tag{15}$$

and substituting (15) in (5) we get

$$\begin{aligned} a_0(t) &= a_0(0) - \frac{c_m}{C}(a_0 - b_0)|_0(1 - e^{-t/\tau}) \\ b_0(t) &= b_0(0) - \frac{c_p}{C}(b_0 - a_0)|_0(1 - e^{-t/\tau}). \end{aligned} \tag{16}$$

for finite wavevector q_n,

$$\begin{aligned} &\dot{a}_n + Dq_n^2 a_n + \frac{c_m}{C\tau}(a_n - b_n) = 0 \\ &\dot{b}_n + vq_n c_n + \frac{c_p}{C\tau}(b_n - a_n) = 0 \\ &\dot{c}_n - vq_n b_n + \frac{c_p}{C\tau}c_n = 0, \end{aligned} \tag{17}$$

By including the time dependence to a_n, b_n, c_n we end up with a system of three ordinary differential equations.Although still coupled , the problem is now computationally easier.Given initial temperature profiles for both $T_p(x,0)$ and $T_m(x,0)$ equations $15-17$ will help investigate the temperature evolution of the above set up.(see Appendix)

6 Results

By numerically solving the dynamic equations we can get valuable insight on the impact the constants in eq (4) have on the temperature evolution of the system.In order to observe the effect a ballistic component has on the phonon temperature profile we will compare it with an uncoupled system where $\tau \to \infty$ by creating the difference $T_{uncoupled} - T_{coupled}$.Because the system depends on four constants and the combinations are numerous we will investigate by fixing three of them at a specific value and only change one at a time.In this way it is certain that any change whatsoever is due to that constant and only.
At first we fix $D = 0.001$, $c_p = 0.9$, $c_m = 0.1$ and vary v.

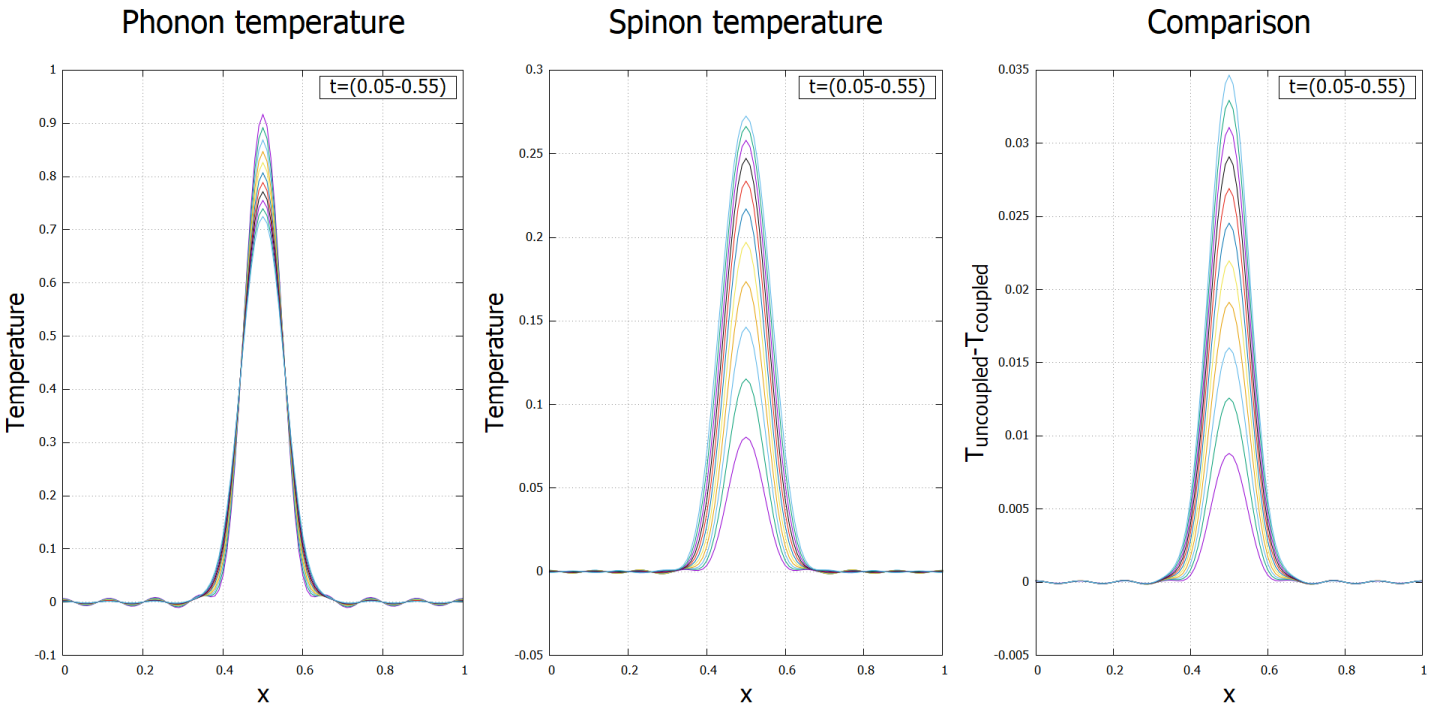
Phonon temperature
Spinon temperature
Comparison
t=(0.05-0.55)
Temperature
T uncoupled-T coupled
x

(a) v=0.1

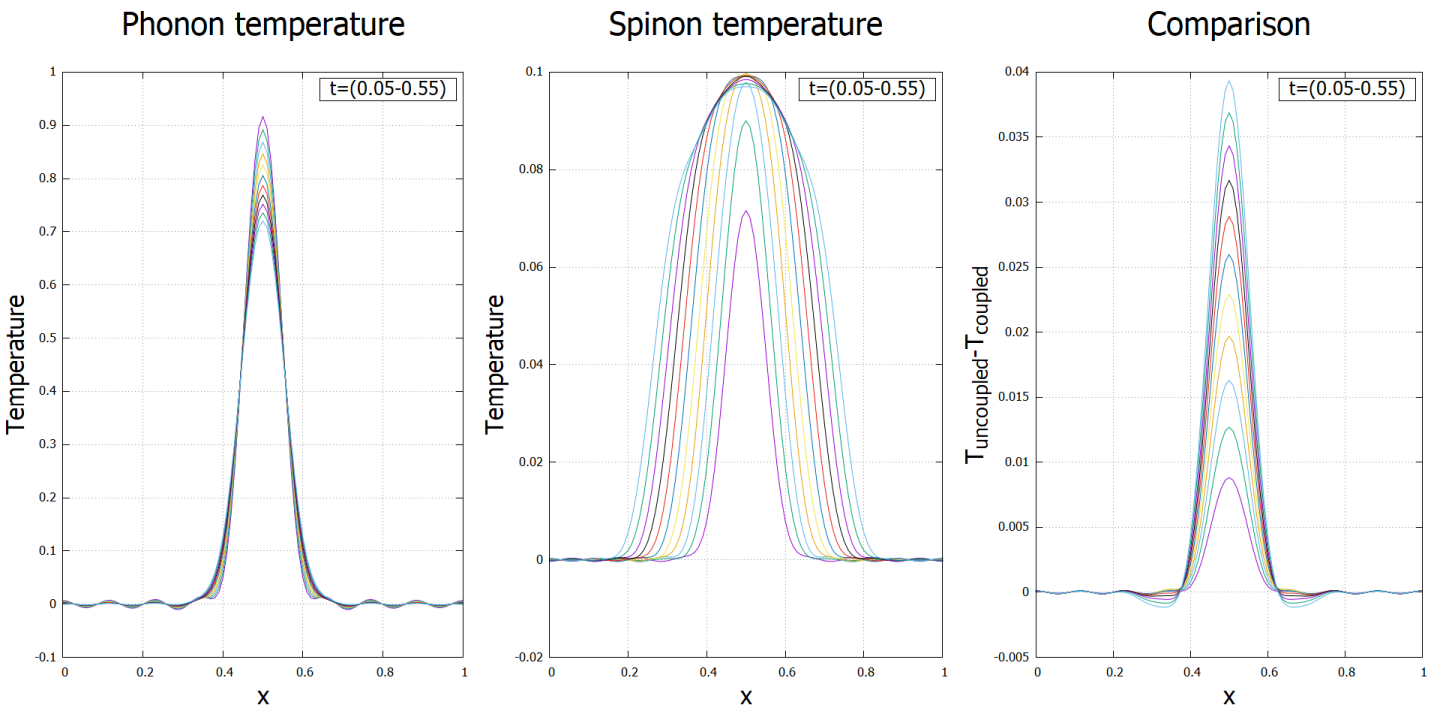
Phonon temperature
Spinon temperature
Comparison
t=(0.05-0.55)
Temperature
T uncoupled-T coupled
x

(b) v=0.4

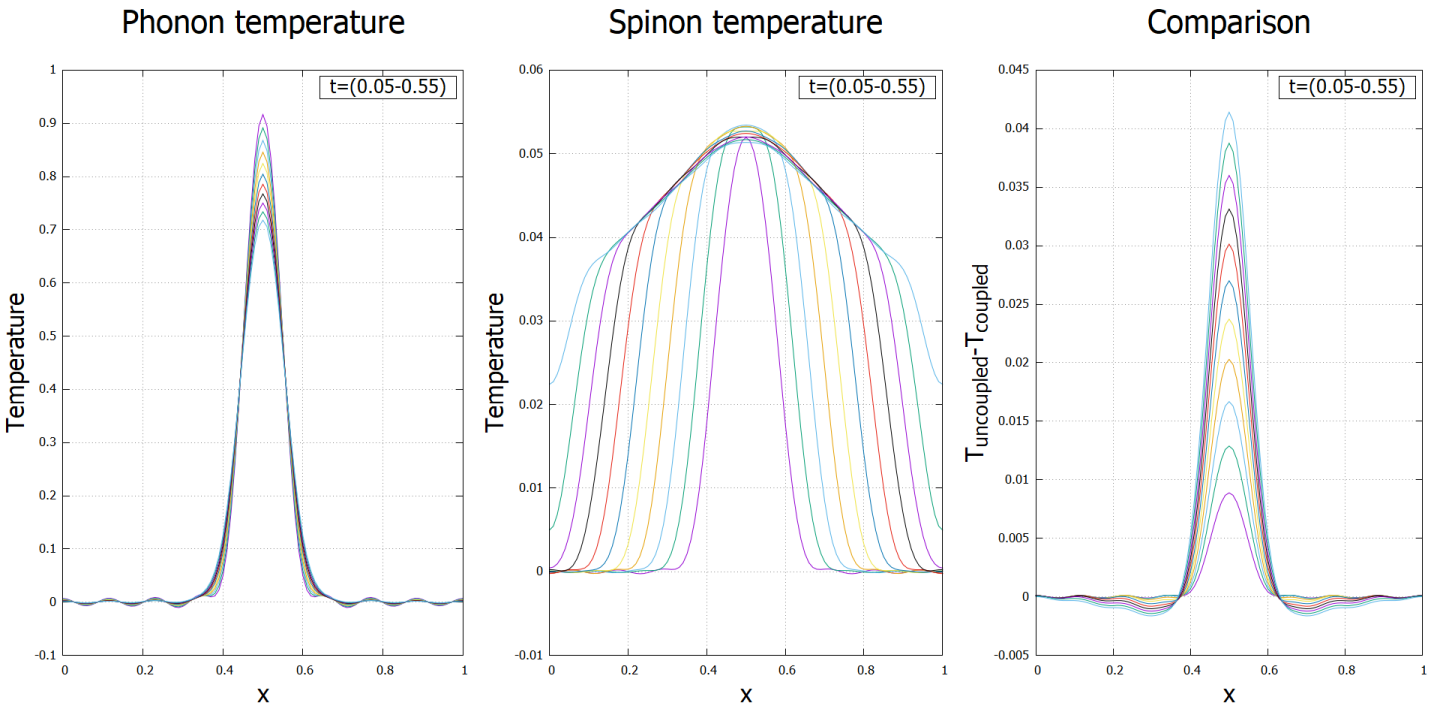

(c) v=0.8

Figure 2: Left to right : Phonon , Magnon , Comparison diagrams for $t[0.005 - 0.55]$

The negative values that appear symmetrically around the center peak at the comparison diagrams confirm that at some point in time the phonon curve is deformed.Additionally the shape of the comparison curve on those intervals highlight the left , right travelling carriers.Because all diagrams are plotted for the same time interval it is easy to see that the greater the velocity the sooner the deformations appear.In Figure 1a negative values do not appear for the simple reason that the carriers haven't yet affected the system.To showcase the connection between the carriers and the time the deformation appears we simply have to check the magnon temperature profile.In both Figure b and c there is significant broadening whereas for Figure a this is not the case.A behaviour like that is expected as the model involves an advection equation which for the homogeneous case has waves as solutions.
Next we fix $c_p = 0.9$, $c_m = 0.1$, $v = 0.5$ and vary D.

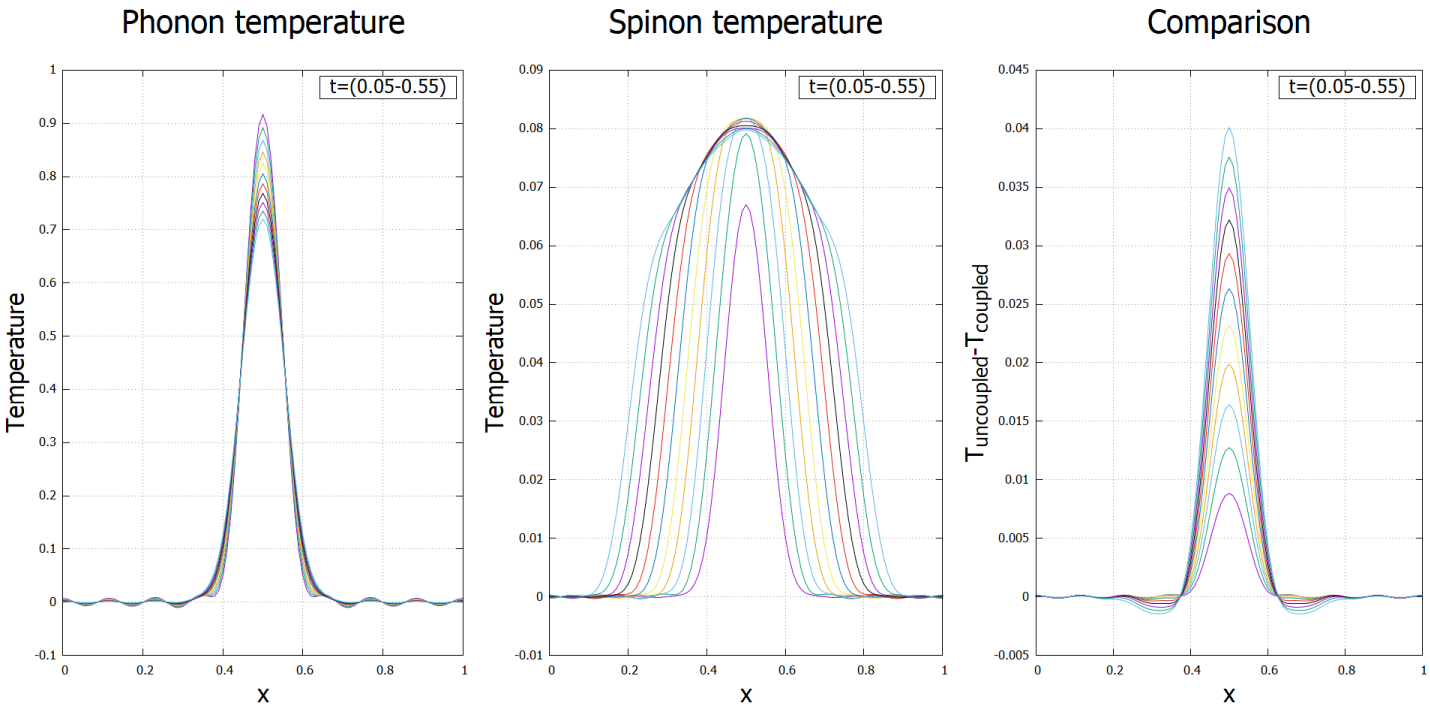

(a) D=0.001

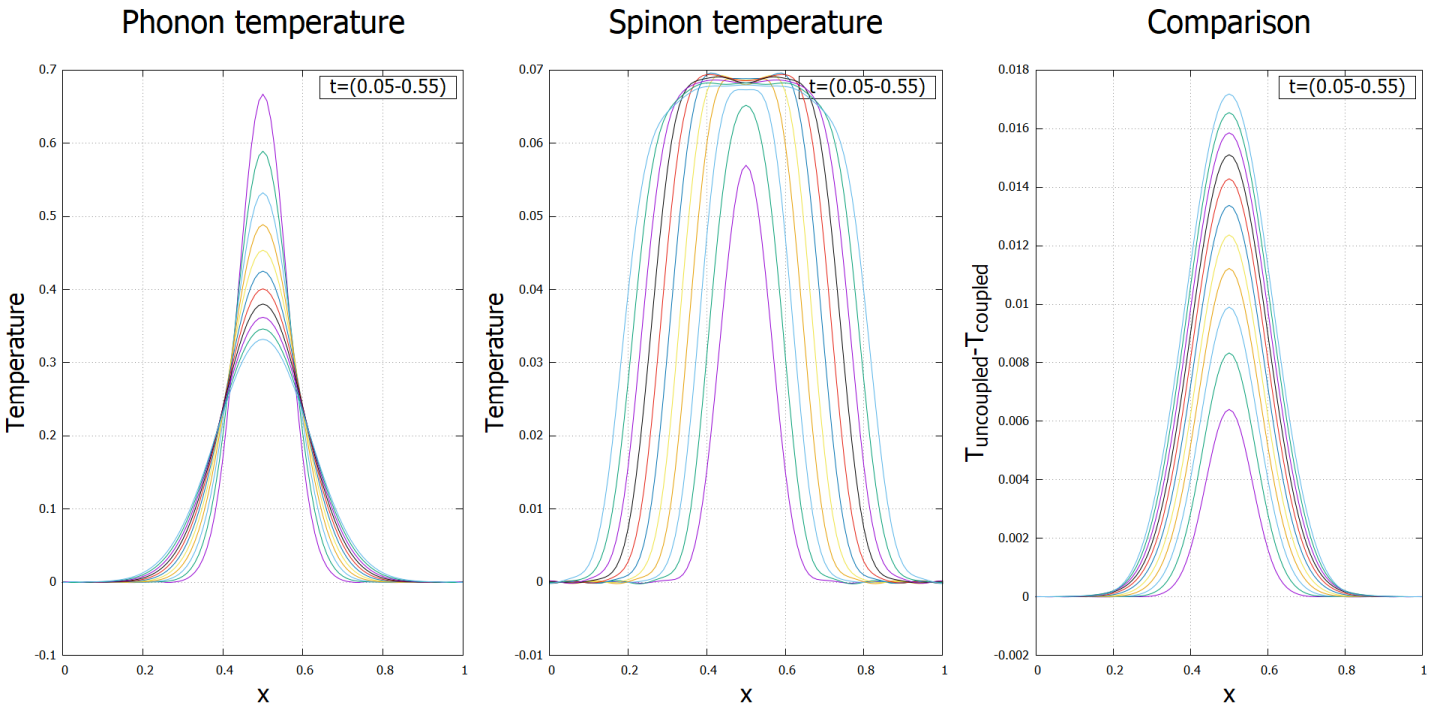

(b) D=0.01

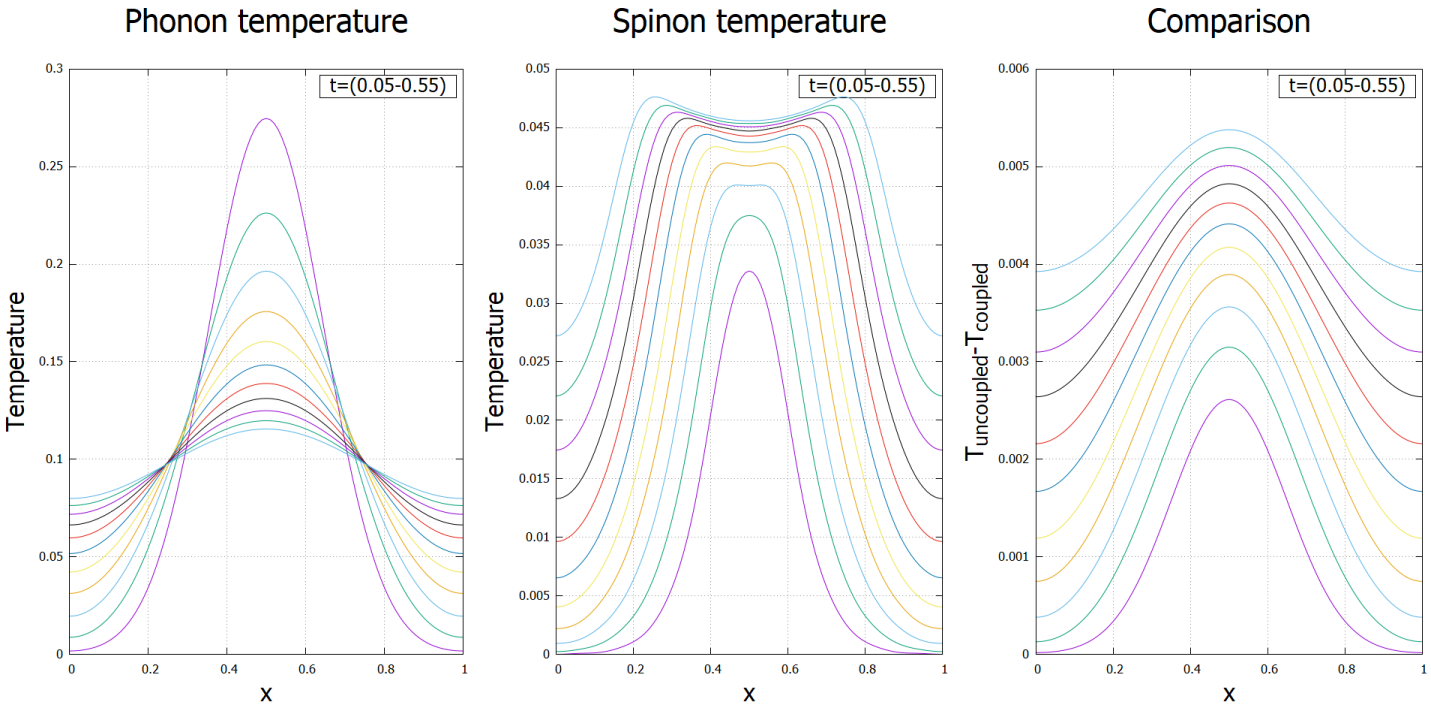

(c) D=0.1

Figure 3: Left to right : Phonon , Magnon , Comparison diagrams for $t[0.005 - 0.55]$

D clearly affects how quickly the temperature drops.From the corresponding diagrams it can be seen that as D increases the amplitude of the phonon , magnon curve decreases.Furthermore a higher value of D creates much clearer peaks at the magnon profile.This is not the case for the comparison diagram where the deformations completely disappear for $D = 0.1$.

Last we fix $D = 0.01$, $v = 0.8$ and vary both c_p and c_m so that $C = c_p + c_m = 1$ and $c_m \leq c_p$.

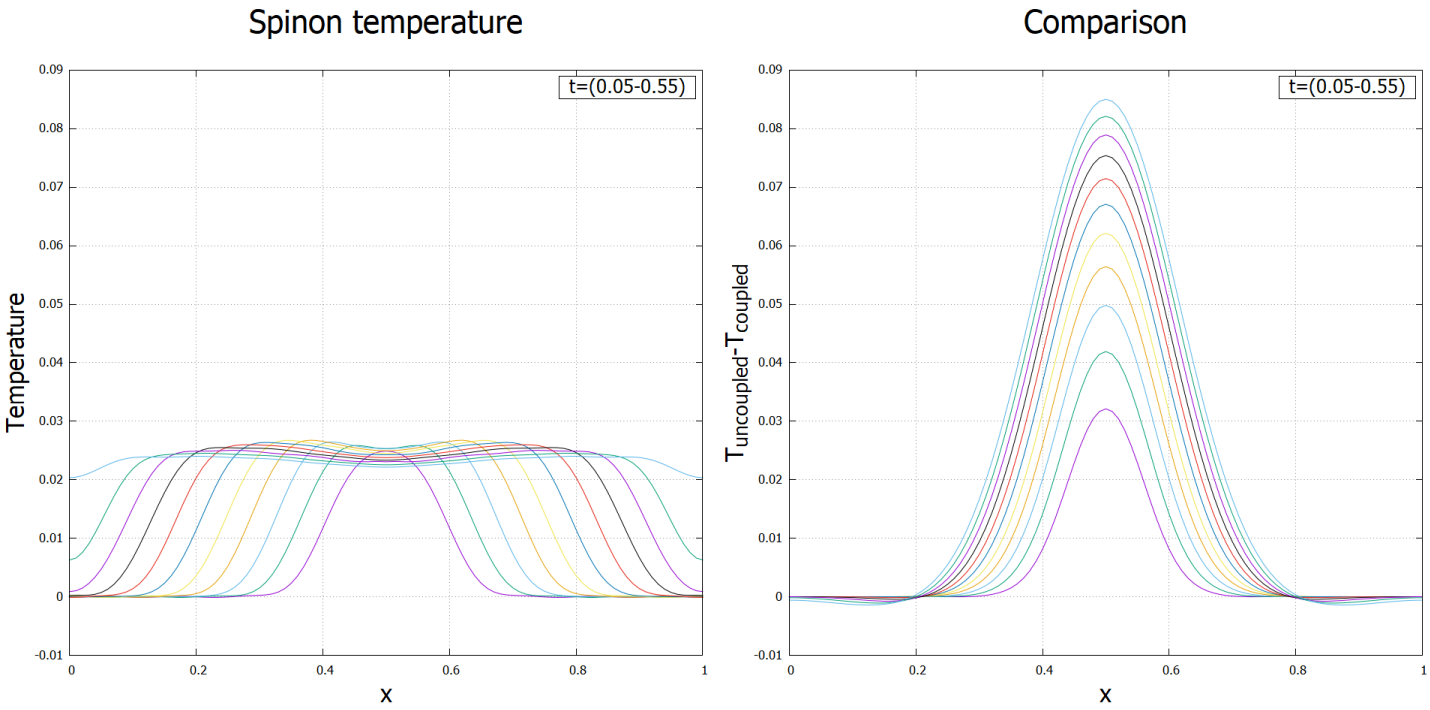

(a) $c_p = 0.5/c_m = 0.5$

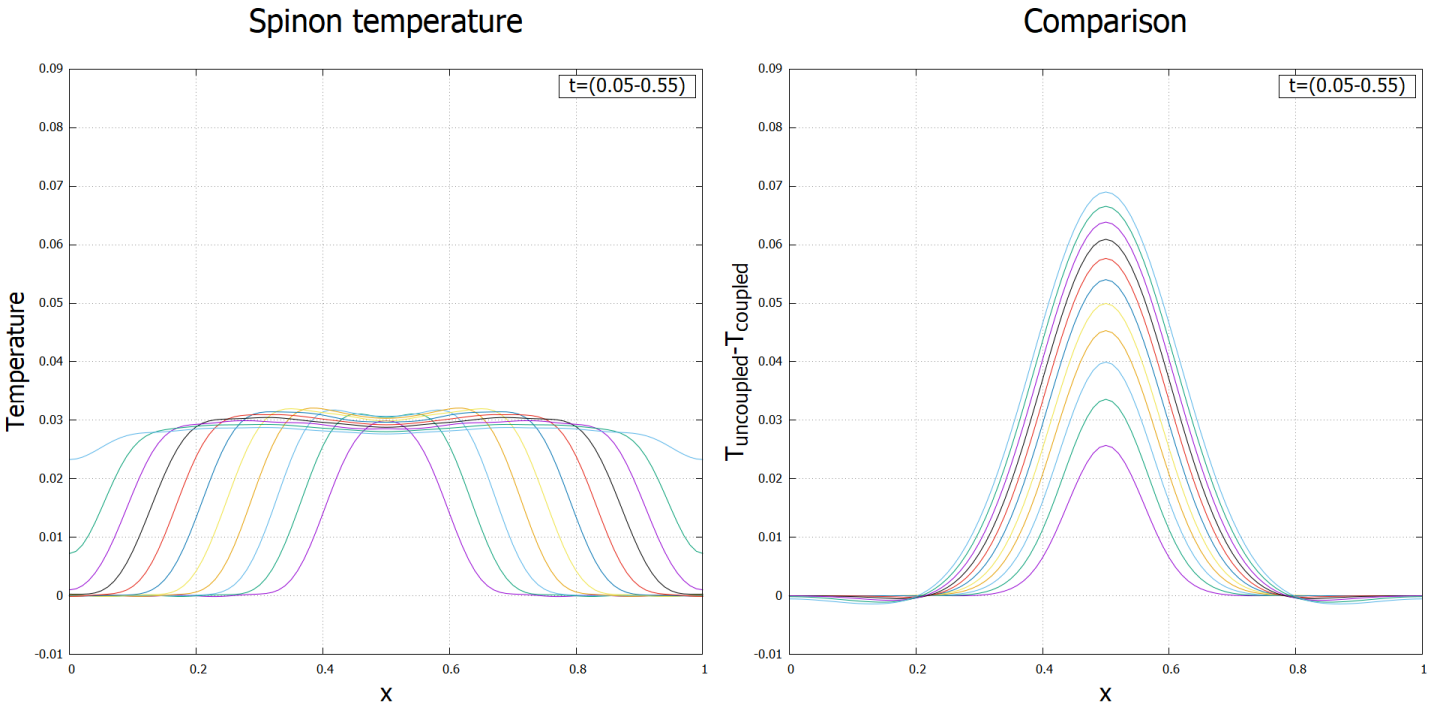

(b) $c_p = 0.6/c_m = 0.4$

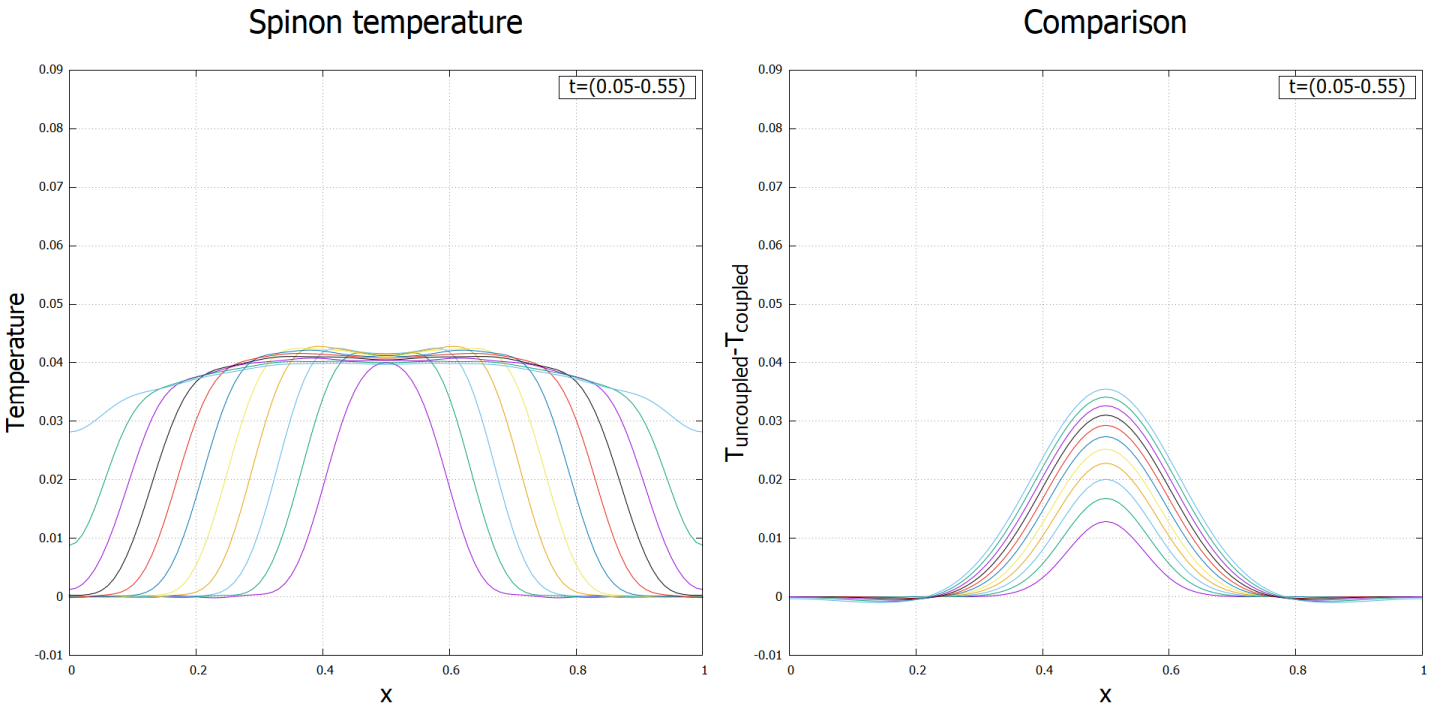

(c) $c_p = 0.8/c_m = 0.2$

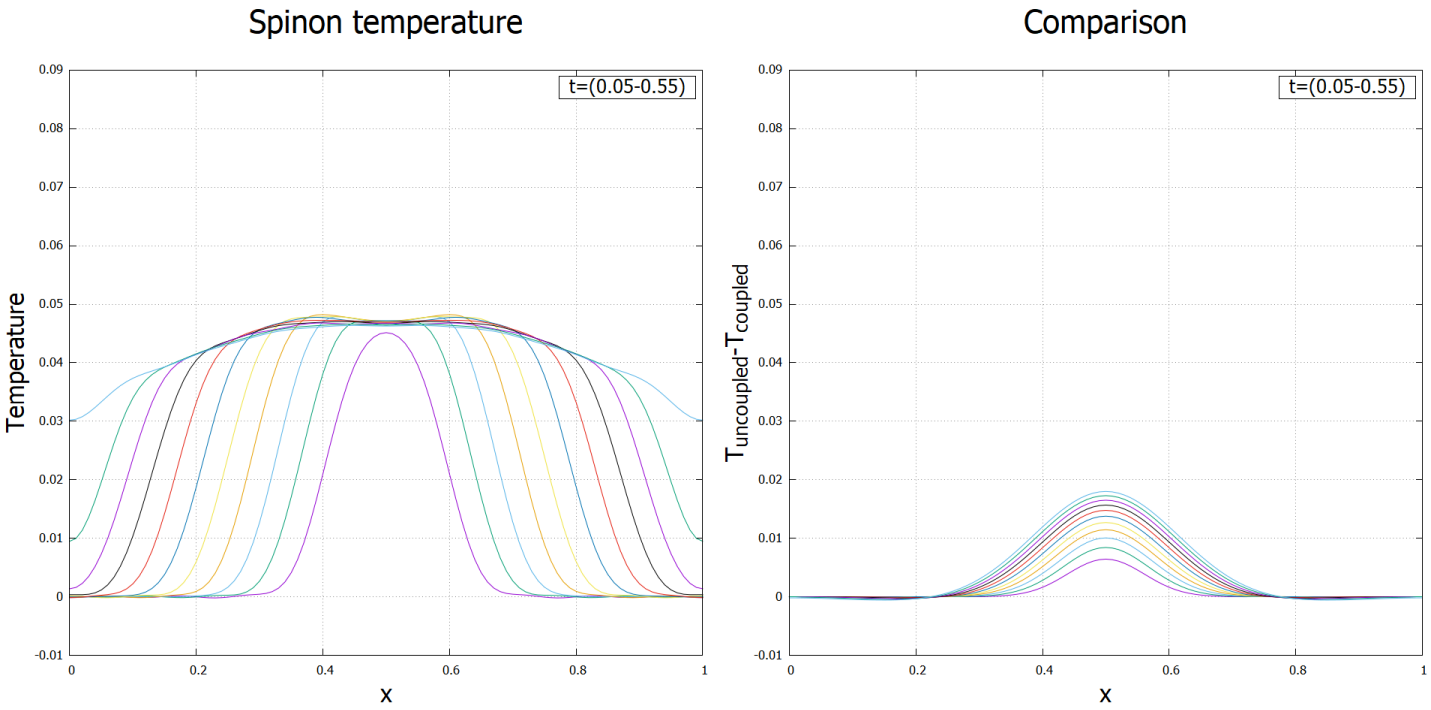

(d) $c_p = 0.9/c_m = 0.1$

Here all diagrams are plotted to the same scale.As the ratio c_p/c_m grows larger than 1 the deformations appearing in the comparison curve tend to disappear.In other words for $c_p/c_m >> 1$ the effect of the ballistic component on the phonon curve is negligible.From another point of view the inhomogeneous term that allows the subsystems to communicate depends on c_m and c_p for the phonon and spinon system respectively.Departure from the homogeneous case of a diffusion equation is due to that term.As the comparison diagrams are a convenient way to check this concept it can be seen that the deformations scale accordingly to c_m.Respectively the amplitude of the magnon diagrams scales with c_p.

7 Conclusion

To recapitulate , as ballistic thermal transport is theorized to occur along the chain or ladder axis we replace the magnon diffusion equation of the two diffusion model with an advection one while assuming a two spinon scattering process.From a phenomenological point of view , the whole investigation of this set up aims at a phonon temperature profile with 3 peaks.One in the center where the material is heated and two others created at a later time due to the spinon-phonon interaction.These appear as deformations rather than distinct peaks.Comparing the coupled system with an uncoupled one is a convenient way to study those deformations.As a comparison between the coupled and the uncoupled system is also experimentally possible , computationally solving the dynamic equations provides valuable information and insight on heat propagation but most importantly reveals how the constants affect the system.As experimental evidence of ballistic thermal transport remains elusive, guidelines based on the above results can be drawn.Ballistic behaviour is best seen when D is small , v is large and the ratio c_p/c_m approaches 1.Materials that satisfy the above requirements could be used to directly observe ballistic thermal transport in a thermal conductivity experiment using the above analysis.

8 Appendix

All calculations were performed using $L = 1$, $C = 1$, $\tau = 1$. The initial profiles chosen for the phonon and spinon subsystems are

$$T_p(x,0) = exp(-300(x-0.5)^2)$$

$$T_{\pm}(x,t) = 0$$

To obtain the Fourier series of $T_p(x.0)$ we use :

$$a_n(0) = 2\int_0^1 cos(q_n x)T_p(x,0)dx$$

Numeric integration was performed in order to find a_0.Equation (16) was used to time evolve a_0 , b_0.For $n[1-17]$ the initial Fourier constants were set as initial conditions to eqs. (17) that were then solved using a 4th order Runge-Kutta method.For each time step , temperature profiles were reconstructed by inverting the Fourier transform.

Listing 1: C++ code

```
#include <iostream>
#include <vector>
#include <fstream>
#include <cmath>
#include <iomanip>
using namespace std;

//simple diffusion  :Limit 1/tau-->inf
double fkd(double x,double dqt)
{
    return -dqt*x;
}
void ruku_nd(int n,double h,double pi,vector <double> & acd,double dqt,double k1,double k2,double
{

    for(int i{0};i<n;i++)
        {
            dqt=d*pow(pi*i,2);
            k1=h*fkd(acd[i],dqt);
            k2=h*fkd(acd[i]+k1/2,dqt);
            k3=h*fkd(acd[i]+k2/2,dqt);
            k4=h*fkd(acd[i]+k3,dqt);
            acd[i]=acd[i]+(1.0/6.0)*(k1+2*k2+2*k3+k4);
        }
        return;
}

//Runge Kutta
double fk(double x,double y,double dqt,double cm)
```

```
30 {
31     return -dqt*x-cm*(x-y);
32 }
33 double fl(double x,double y,double z,double vqt,double cp)
34 {
35     return -vqt*z-cp*(y-x);
36 }
37 double fm(double y,double z,double vqt,double cp)
38 {
39     return vqt*y-cp*(z);
40 }
41 void ruku_n(int n,double h,double pi,vector <double> & ac,vector <double> & bc,
42 vector <double> & cc,double cm,double cp,double vqt,double dqt,
43 double k1,double k2,double k3,double k4,double l1,double l2,double l3,
44 double l4,double m1,double m2,double m3,double m4,double d,double v)
45 {
46
47     for(int i{1};i<n;i++)
48         {
49             dqt=d*pow(pi*i,2);
50             vqt=v*pi*i;
51
52
53             k1=h*fk(ac[i],bc[i],dqt,cm);
54             l1=h*fl(ac[i],bc[i],cc[i],vqt,cp);
55             m1=h*fm(bc[i],cc[i],vqt,cp);
56
57             k2=h*fk(ac[i]+k1/2,bc[i]+l1/2,dqt,cm);
58             l2=h*fl(ac[i]+k1/2,bc[i]+l1/2,cc[i]+m1/2,vqt,cp);
59             m2=h*fm(bc[i]+l1/2,cc[i]+m1/2,vqt,cp);
60
61             k3=h*fk(ac[i]+k2/2,bc[i]+l2/2,dqt,cm);
62             l3=h*fl(ac[i]+k2/2,bc[i]+l2/2,cc[i],vqt,cp);
63             m3=h*fm(bc[i]+l2/2,cc[i]+m2/2,vqt,cp);
64
65             k4=h*fk(ac[i]+k3,bc[i]+l3,dqt,cm);
66             l4=h*fl(ac[i]+k3,bc[i]+l3,cc[i]+m3,vqt,cp);
67             m4=h*fm(bc[i]+l3,cc[i]+m3,vqt,cp);
68
69             ac[i]=ac[i]+(1.0/6.0)*(k1+2*k2+2*k3+k4);
70             bc[i]=bc[i]+(1.0/6.0)*(l1+2*l2+2*l3+l4);
71             cc[i]=cc[i]+(1.0/6.0)*(m1+2*m2+2*m3+m4);
72         }
73         return;
74 }
75
76 void time_evolution0(vector <double> & ac,vector <double> & bc,vector <double> & cc,
77 double a0,double b0,double c0,double t,double cp,double cm)
78 {
79     ac[0]=a0-cm*(a0-b0)*(1.0-exp(-t));
80     bc[0]=b0-cp*(b0-a0)*(1.0-exp(-t));
81     cc[0]=c0;
82 }
83
84 //Simpson integration
85 double f(double x,int n,double pi)
86 {
87     return 2*exp(-300.0*(x-0.5)*(x-0.5))*cos(pi*n*x);
88 }
89 double intergal(double a,double b,int divisions,int n,double pi)
```

```
90  {
91      double h=(b-a)/divisions;
92      double s=(f(a,n,pi)+f(b,n,pi));
93      for(int i{1};i<=divisions-1;i+=2)
94          {
95              s+= 4*f(a+i*h,n,pi);
96          }
97      for(int i{2};i<=divisions-2;i+=2)
98          {
99              s+=2*f(a+i*h,n,pi);
100         }
101
102     return (h/3)*s;
103 }
104
105
106
107 int main()
108 {
109     const double pi=3.141592653589793238463;
110     int constexpr n=17;                                    // number of fourier const.
111     int xmax=100.0;
112     double dx=0.01;
113     double x0=0.0;
114     int m=10000;  //time steps
115     double h=0.001;
116     double dqt{0},vqt{0};
117     double d{0.1};
118     double v{1.0};
119     double cm=0.1;
120     double cp=0.9;
121     double k1{0},k2{0},k3{0},k4{0},l1{0},l2{0},l3{0},l4{0},m1{0},m2{0},m3{0},m4{0};
122     double t=0;
123
124     vector<double> ac(n),bc(n,0),cc(n,0),acd(n);
125
126     //simpson
127     int divisions=100;
128     double a=0.0;
129     double b=1.0;
130     for(int k{0};k<n;k+=1)
131         {
132             ac[k]=intergal(a,b,divisions,k,pi);
133             acd[k]=intergal(a,b,divisions,k,pi);
134         }
135
136     //iversion
137     double const a0=ac[0];
138     double const b0=bc[0];
139     double const c0=0.0;
140
141     double difftemp{0};
142     double phtemp{0};
143     double mptemp{0};
144     double mmtemp{0};
145     double energy{0},phenergy{0},magenergy{0};
146
147     ofstream ph;
148     ph.open ("phtemp.txt");
149     ofstream mg;
```

```
150     mg.open ("magtemp.txt");
151     ofstream sy;
152     sy.open ("system.txt");
153     ofstream en;
154     en.open ("energy.txt");
155     ofstream pic;
156     pic.open ("profile.txt");
157     ofstream tem;
158     tem.open ("temperature.txt");
159
160
161     for(int j{0};j<m;j++)
162         {
163             t=h*j;
164             if(j!=0)
165             {
166                 time_evolution0(ac,bc,cc,a0,b0,c0,t,cp,cm);
167                 ruku_n(n,h,pi,ac,bc,cc,cm,cp,vqt,dqt,k1,k2,k3,k4,l1,l2,l3,l4,m1,m2,m3,m4,d,v);
168
169                 ruku_nd(n,h,pi,acd,dqt,k1,k2,k3,k4,d);
170             }
171             for(int k{0};k<=xmax;k++)
172                 {
173                     for(int i{0};i<n;i++)
174                         {
175                             if(i==0)
176                             {
177                                 phtemp += 0.5*ac[i];
178                                 mptemp += 0.5*bc[i];
179                                 mmtemp += 0.5*bc[i];
180                                 difftemp +=0.5*acd[i];
181                             }else{
182                                 phtemp += ac[i]*cos(i*pi*(x0+k*dx));
183                                 mptemp += bc[i]*cos(i*pi*(x0+k*dx))+cc[i]*sin(i*pi*(x0+k*dx));
184                                 mmtemp += bc[i]*cos(i*pi*(x0+k*dx))-cc[i]*sin(i*pi*(x0+k*dx));
185                                 difftemp +=acd[i]*cos(i*pi*(x0+k*dx));
186                             }
187
188                         }
189
190                     ph<<x0+k*dx<<' '<<phtemp<<' '<<(difftemp-phtemp)<<' '<<t<<endl;
191                     mg<<x0+k*dx<<' '<<0.5*(mptemp+mmtemp)<<' '<<t<<endl;
192                     sy<<x0+k*dx<<' '<<phtemp+0.5*(mptemp+mmtemp)<<' '<<t<<endl;
193
194                     if(j>40){
195                     if((j%50==0)&&(j<m))
196                     {
197                    pic<<t<<' '<<x0+k*dx<<' '<<phtemp+0.5*(mptemp+mmtemp)
198                    <<' '<<0.5*(mptemp+mmtemp)<<' '<<phtemp<<' '<<abs(difftemp-phtemp)<<endl;
199                     }
200                     }
201
202                     phenergy+=dx*cp*phtemp;
203                     magenergy+=dx*cm*(mptemp+mmtemp)*0.5;
204                     energy+=dx*(cp*phtemp+cm*0.5*(mptemp+mmtemp));
205
206                     phtemp=0;
207                     mptemp=0;
208                     mmtemp=0;
209                     difftemp=0;
```

```
210
211                     }
212
213                     en<<t<<' '<<phenergy<<' '<<magenergy<<' '<<energy<<endl;
214                     tem<<t<<' '<<phenergy/cp<<' '<<magenergy/cm<<' '<<phenergy/cp+magenergy/cm<<endl
215
216                     ph<<endl<<endl;
217                     mg<<endl<<endl;
218                     sy<<endl<<endl;
219
220                     if(j>40){
221                     if((j%50==0)&&(j<m))
222                     {
223                             pic<<endl<<endl;
224                     }
225                     }
226
227                     phenergy=0;
228                     magenergy=0;
229                     energy=0;
230
231             }
232     return 0;
233     }
```

In order to test the validity of the program a simple check can be done.With zero energy current boundary conditions the total energy of the system should remain constant.Calculating energy as the area under the temperature curve for each time step we plot the corresponding diagram :

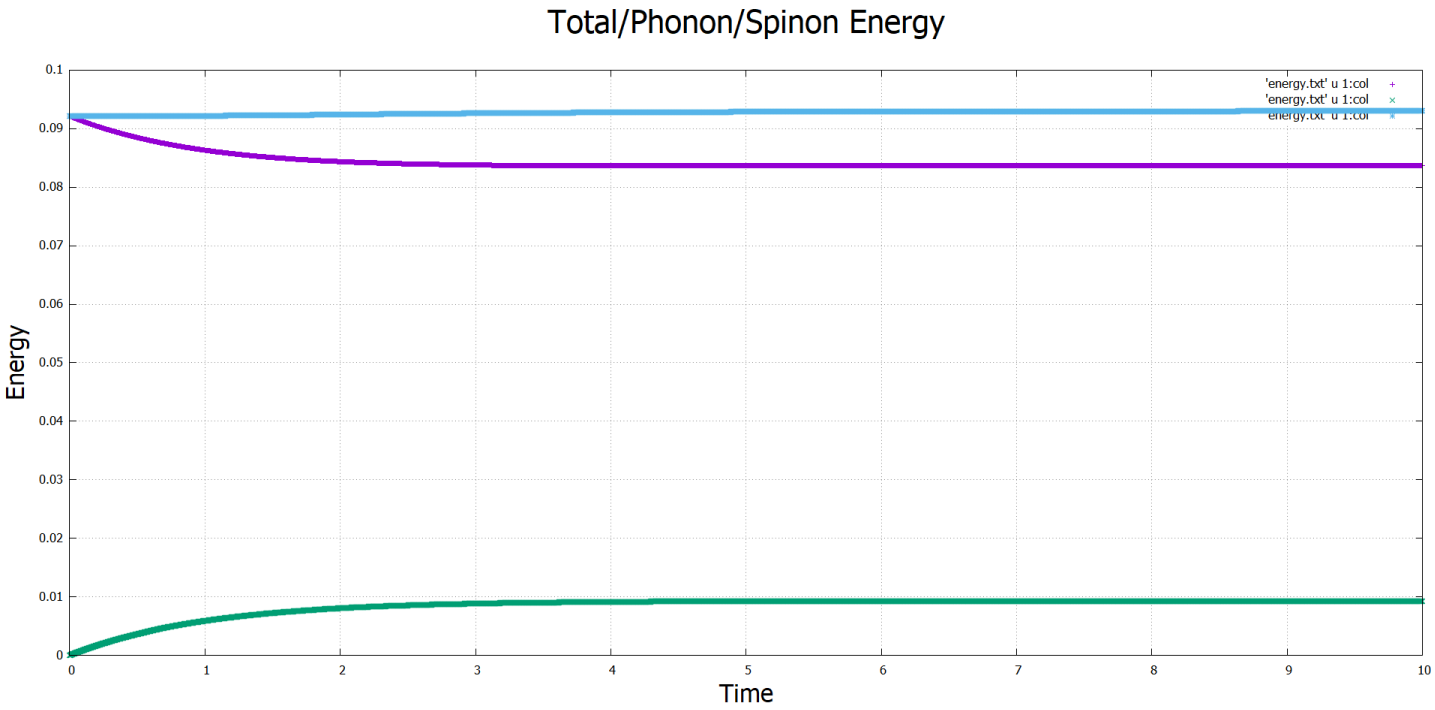

Figure 5: Blue:Total energy /Purple:Phonon energy /Green:Spinon energy

It can be seen that overall the energy remains constant , taking into account that throughout the calculations we used an approximation method.

References

[1] X. Zotos, F. Naef, and P. Prelovsek, "Transport and conservation laws," *Physical Review B*, vol. 55, no. 17, p. 11029, 1997.

[2] C. Hess, "Heat transport of cuprate-based low-dimensional quantum magnets with strong exchange coupling," *Physics Reports*, vol. 811, pp. 1–38, 2019.

[3] W. J. Parker, R. J. Jenkins, C. P. Butler, and G. L. Abbott, "Flash method of determining thermal diffusivity, heat capacity, and thermal conductivity," *Journal of Applied Physics*, vol. 32, no. 9, pp. 1679–1684, 1961.

[4] D. J. Sanders and D. Walton, "Effect of magnon-phonon thermal relaxation on heat transport by magnons," *Phys. Rev. B*, vol. 15, pp. 1489–1494, Feb 1977.

[5] M. Montagnese, M. Otter, X. Zotos, D. A. Fishman, N. Hlubek, O. Mityashkin, C. Hess, R. Saint-Martin, S. Singh, A. Revcolevschi, and P. H. M. van Loosdrecht, "Phonon-magnon interaction in low dimensional quantum magnets observed by dynamic heat transport measurements," *Phys. Rev. Lett.*, vol. 110, p. 147206, Apr 2013.